Journal of Photochemistry & Photobiology, B: Biology 177 (2017) 8–17

Contents lists available at ScienceDirect

Journal of Photochemistry & Photobiology, B: Biology

journal homepage: www.elsevier.com/locate/jphotobiol

A comprehensive analysis of direct and photosensitized attenuation of *Toxoplasma gondii* tachyzoites

Juan G. Yañuk[a], M. Lis Alomar[a], M. Micaela Gonzalez[a], Andrés M. Alonso[b], Sergio O. Angel[b], Verónica M. Coceres[b], Franco M. Cabrerizo[a,*]

[a] *Laboratorio de Fotoquímica y Fotobiología Molecular, Instituto de Investigaciones Biotecnológicas - Instituto Tecnológico de Chascomús (IIB-INTECH), Universidad Nacional de San Martín (UNSAM) - Consejo Nacional de Investigaciones Científicas y Técnicas (CONICET), Av. Intendente Marino Km. 8.2, C.C 164, B7130IIWA Chascomús, Prov. Buenos Aires, Argentina*

[b] *Laboratorio de Parasitología Molecular, Instituto de Investigaciones Biotecnológicas - Instituto Tecnológico de Chascomús (IIB-INTECH), Universidad Nacional de San Martín (UNSAM) - Consejo Nacional de Investigaciones Científicas y Técnicas (CONICET), Av. Intendente Marino Km. 8.2, C.C 164, B7130IIWA Chascomús, Prov. Buenos Aires, Argentina*

ABSTRACT

In the present work, we have evaluated the effect of three different types of radiation: UVC (254 ± 5 nm), UVA (365 ± 20 nm) and visible (420 ± 20 nm) on different morphological and biological functions of *Toxoplasma gondii* tachyzoites. Briefly, UVC and UVA showed an inhibitory effect on parasite invasion in a dose-dependent manner. UVC showed the strongest effect inducing both structural damage (antigens) and functional inhibition (*i.e.*, invasion and replication). On its own, visible light induces a quite distinctive and selective pattern of parasite-attenuation. This type of incident radiation inhibits the replication of the parasite affecting neither the capability of invasion/attachment nor the native structure of proteins (antigens) on parasites. Such effects are a consequence of photosensitized processes where phenol red might act as the active photosensitizer. The potential uses of the methodologies investigated herein are discussed.

1. Introduction

Toxoplasma gondii is a protozoan obligate intracellular parasite that can infect a wide range of animals including humans. This parasite is ubiquitous throughout the world and infect around a third of humans worldwide. Infection can result in severe clinical diseases such as encephalitis and chorioretinitis in immunocompromised hosts [1], chorioretinitis in immunocompetent hosts and serious congenital diseases in developing fetus if pregnant women become infected for the first time during pregnancy [2]. In addition, infection in domestic animals is a threat to public health from food-borne outbreaks and causes a great economic loss as it may lead to abortion, stillbirth and neonatal loss [3]. Therefore, toxoplasmosis is of great medical and veterinary importance.

The success of *T. gondii* infection relies on host cell recognition and attachment, invasion, replication and egress to spread throughout the host organism. Once inside a host, the parasite employs powerful molecular effectors that modulate the host cell, developing into a chronic infection [4]. In addition, current toxoplasmosis treatment is limited because of its side effects and inefficiency against tissue cysts [5]. Thus, the development of an effective vaccine against this parasite would decrease the enormous costs of diagnosis/treatment, the premature loss of lives, the extensive rates of dissemination as well as the social impact of the disease.

At present, there is only one commercial vaccine (Toxovax), based on live attenuated S48 strain, that has been licensed to be used to avoid congenital infection in ewes [6]. However, this vaccine may revert to a pathogenic strain and, therefore, it is not suitable for human use. Moreover, there is currently no licensed vaccine available for humans.

It is well known that vaccines based on live-attenuated parasites are more efficient than vaccines based on dead-parasites, because the former ones emulates the natural infection, mobilizing a MHC class I-restricted CD 8 + T-cell response [7]. In the particular case of intracellular parasites, an efficient vaccine should be made of attenuated parasites that can invade but cannot replicate inside the host cell, preserving the integrity of the antigens and therefore, providing protective immunity.

Many strategies have been followed to achieve such a goal. In particular, γ, X-ray and ultraviolet type C (UVC) radiation have been used as attenuation sources of a remarkably wide range of parasite species. Immunization of laboratory animals with various irradiated

* Corresponding author.
E-mail address: fcabrerizo@intech.gov.ar (F.M. Cabrerizo).

http://dx.doi.org/10.1016/j.jphotobiol.2017.10.008
Received 27 July 2017; Received in revised form 26 September 2017; Accepted 5 October 2017
Available online 07 October 2017
1011-1344/

protozoan parasites, including species of *Plasmodium* [8], *Leishmania* [9,10], *Trypanosoma* [11], *Toxoplasma gondii* [12–15], *Neospora caninum* [16], among others, has been reported. In every case, irradiated parasites induce protective immunity against subsequent challenge of experimental hosts [9,16–18].

The apparent success of UVC- and/or γ-attenuated vaccine relies on the changes on the conformation and presentation of parasite antigens induced by the radiation that may be crucial in enhancing parasite immunogenicity [17]. However, the mechanisms through which the above mentioned radiations interact with cellular processes are still poorly understood and somewhat controversial. In the case of *T. gondii*, this lack of understanding is due to the fact that *in vitro* studies employ different parasite models (*i.e.*, tachyzoites or oocystes), end points and, most fundamentally, different experimental parameters (*i.e.*, radiation sources and exposure media) [12–14].

Parasite's attenuation may be either due to direct absorption of the incident radiation by molecular targets (DNA, proteins, nucleotides, amino acids, lipids, *etc.*) or mediated by reactive oxygen species (produced by radiolysis of water, among other sources) leading to a highly oxidant environment. Such an environment can certainly induce unspecific and uncontrollable damage on both morphological and functional aspects of the parasites. Thus, the type and/or extent of damage and, consequently, the immunogenicity, would depend on the UVC doses applied [17]. Therefore, other attenuation sources such as ultraviolet type A (UVA) and visible radiation, *via* photosensitization, should be taken into account and further evaluated.

In the present work, a systematic and comparative evaluation of the effect of three different types of radiation (UVC, UVA and visible) as attenuation sources of *T. gondii* tachyzoites has been carried out. In particular, we have evaluated the effect on morphological (shape and size), antigenic properties of different proteins, intracellular Reactive Oxygen Species (ROS) production and physiological functions (invasion and replication capability) of the parasite.

2. Experimental

2.1. Parasite Source, Culture and Manipulation

Tachyzoites (Tz) of RH strain were cultured in standard conditions *in vitro*: Vero (Epithelial Kidney *Cercopithecus aethiops*) and HFF (human foreskin fibroblast) cell monolayers were infected with tachyzoites and incubated with Dulbecco's modified Eagle medium (DMEM, Gibco BRL) supplemented with 5 or 10% fetal bovine serum, penicillin (100 UI/mL; GIBCO) and streptomycin (100 μg/mL; GIBCO) at 37 °C, in a humidified 5% CO_2 atmosphere.

2.2. Parasite Treatments and/or Attenuation

2.2.1. Irradiation of Tachyzoites (Irradiated-Tz) Under Extracellular Conditions

7×10^7 tachyzoites (counted in a Neubauer hemocytometer chamber) were centrifuged for 10 min at 800 × *g*. The pellet was dissolved in 3 mL of phosphate buffer solution (PBS). Parasite suspension were then irradiated at different times (up to 50 min) in a quartz cell (10 mm optical path length), at a fixed distance (1 cm) from the source, at room temperature. Three different types of irradiation sources were investigated: UVC (254 ± 5 nm, 0.17 mW/cm^2), UVA (365 ± 20 nm, 2.1 mW/cm^2) and a Rayonet lamp as a source of visible light (420 ± 20 nm, 6.4 mW/cm^2). Corresponding emission spectra are presented in Supplementary information (Fig. SI.1). All irradiances were measured by a USB2000 (Ocean Optics) calibrated spectroradiometer.

2.2.2. Photosensitized Attenuation of Tachyzoites: Effect of Phenol Red (PR)

For this purpose, three independent sets of parasites were grown in DMEM media containing three different PR concentrations (0, 0.04 and 0.40 mM, respectively). High PR DMEM (0.40 mM) was obtained by adding PR (*Sigma-Aldrich*) to commercial PR DMEM (0.04 mM). After two consecutive cycles of invasion, replication and lysis, typically 7×10^7 tachyzoites were washed with PBS and centrifuged at room temperature for 10 min at 800 × *g*. Pellets were dissolved in 3 mL of PBS and exposed to visible light, at room temperature, during different intervals of time (see Section 2.2.1).

2.3. Microscopy

An epifluorescence microscope Nikon Eclipse E-600 was used. Fluorescence imaging experiments were performed by irradiating the cells and their surroundings with a super high pressure mercury lamp (model HB-10104AF, Nikon Corp) using bandpass filters to select the wavelength appropriate for excitation. Light emitted by the sample was detected through a bandpass filter appropriate for each experiment using a Nikon DS-Qi1Mc camera (controlled by NIS-Elements software version 4.0, Nikon Corp.). Phase-contrast images were recorded using the same camera; back-lighting was achieved with a tungsten lamp. All microscopic images were acquired with a 100 × oil-immersion objective.

2.4. Invasion

Invasion experiments were done by:

2.4.1. Indirect Immunofluorescence Assay (IFA)

Untreated (control) and treated-Tz (4×10^6) were added to Vero cell monolayers grown in 24 well plates on glass coverslips, incubated 10 min on ice and after that at 37 °C during 1 h, washed three times with PBS and fixed with 4% paraformaldehyde. Finally, samples were permeabilized with 0.2% Triton X-100 (Sigma-Aldrich) and incubated with anti-*T. gondii* P30 (SAG1) mouse-monoclonal antibody (Novus Biologicals, 1:50) for 1 h at room temperature. After washing with PBS, cells were incubated with Alexa Fluor® 488-conjugated anti-mouse IgG goat antibody (Invitrogen, 1:4000) during 1 h at room temperature in dark. Fifty random fields (Section 2.3) with similar number of host cells were analyzed, under microscope, in duplicate in three independent sets of experiments. Data are presented as means of parasitophorous vacuoles per field (PV/field) ± SD.

2.4.2. Red/Green Assay

Immunofluorescence staining was performed following the steps described in Section 2.4.1 with modifications [19]. Briefly, after monolayers were fixed, external (attached) tachyzoites were stained with anti-SAG1 rabbit-polyclonal (1:100)/goat anti-rabbit Alexa Fluor® 594 (Invitrogen, 1:4000) antibodies. Then, samples were permeabilized and incubated with anti-SAG1 mouse-monoclonal/goat anti-mouse Alexa Fluor® 488 (Invitrogen, 1:4000) antibodies, for detection of internal tachyzoites (Fig. SI.2(a)). The difference between the number of parasites detected with anti-SAG1 mouse-monoclonal and that detected by anti-SAG1 rabbit-polyclonal antibodies represents the number of parasites inside the host cell. Twenty randomly selected fields (with an average of 250 total tachyzoites) were analyzed, in duplicate, in three independent sets of experiments. Only fields with similar number of host cells were taken into account. Results are expressed as means of attached (in red) and internal (green) tachyzoites per field ± SEM, grouped in stacked columns.

2.5. Replication

The replication rate was determined by incubating untreated and treated-Tz (4×10^6) with Vero cell monolayers, incubated 10 min on ice and after that at 37 °C during 1 h and washed three times with PBS. Finally, samples were incubated an additional 16 or 24 h with fresh

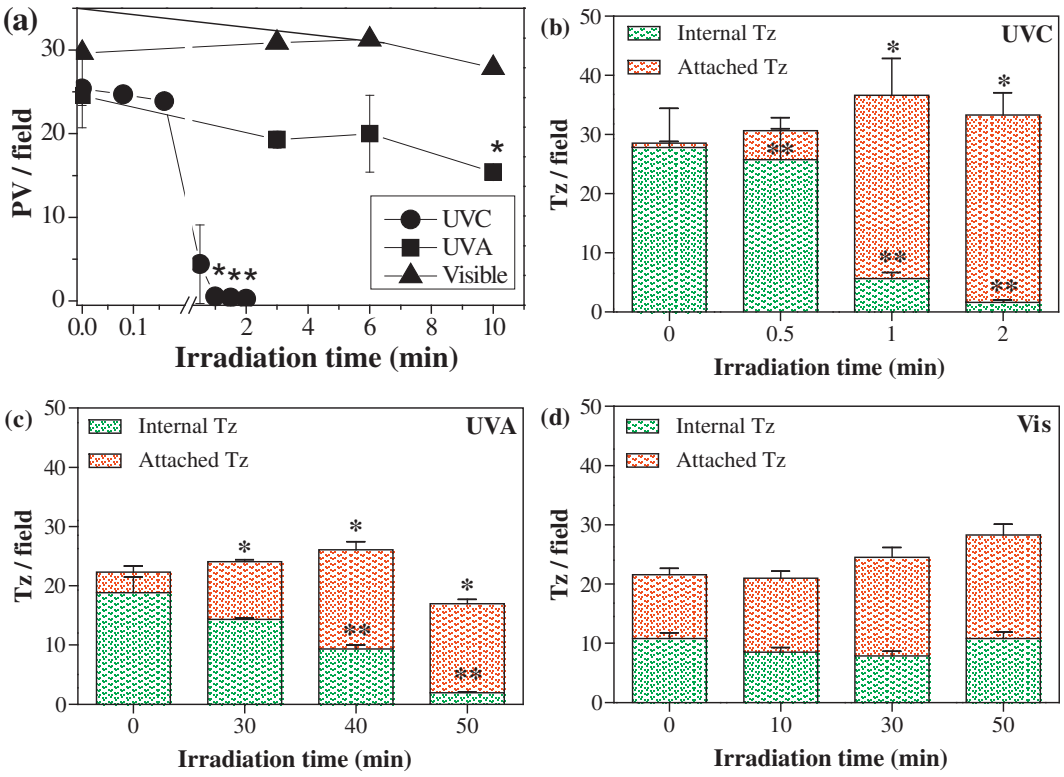

Fig. 1. Effects of UVC, UVA and visible radiation on parasite's invasion. Extracellular tachyzoites were irradiated with different type of radiation during various irradiation times and allowed to invade Vero cells monolayers. Samples were analyzed by: (a) IFA assay (used to count number of PV per field in 50 fields). Results are expressed as mean of PV/field ± SD from three independent experiments and were analyzed by Kruskal-Wallis test followed by Dunn's method. * indicates statistically significant differences between irradiated samples and controls without irradiation ($p < 0.05$); (b), (c) and (d) Red/Green IFA assay corresponding to UVC, UVA and visible irradiation, respectively. Data are represented as internal (in green) and attached (red) Tz/field (mean ± SEM from three independent experiments). ** and * indicate statistically significant differences in internal and attached Tz/field, respectively, between irradiated samples and their corresponding controls without irradiation ($p < 0.05$, ANOVA/Dunnett's tests). Non-significant statistical differences were found in total amount of Tz/field. (For interpretation of the references to colour in this figure legend, the reader is referred to the web version of this article.)

DMEM supplemented with 5% FBS, at 37 °C in a 5% CO_2 humidified atmosphere. After the infected monolayers were fixed, they were immunolabeled as was explained in Section 2.4.1. The number of tachyzoites per PV was counted under microscope (Section 2.3). 100 PVs selected at random were counted in duplicate, per each radiation dose, in three independent sets of experiments. Data are presented as the mean percentage of PVs that contained a geometric progression (*e.g.* 1, 2, 4, 8, 16) of tachyzoites per PV ± SEM (Fig. SI.2(b) and (c)).

2.6. Analysis of Tachyzoites' Morphology

Untreated and treated-Tz were added on poly-L-lysine-coated slides for 30 min. Then, phase-contrast microscopic images were acquired (Section 2.3). Circularity and area of tachyzoites were calculated with ImageJ software. Circularity values (calculated as 4π *area / perimeter*^{2}) vary between 0 (that indicates a polygon) and 1 (that corresponds to a perfect circle). 100 tachyzoites randomly selected were analyzed in duplicates, in two independent experiments. Data are presented as means ± SEM.

2.7. Analysis of T. gondii's Antigens

Antigenic properties of different proteins were assayed by western blot. Briefly, 2.5×10^7 tachyzoites were irradiated in a 10 × 10 mm quartz cell, using the irradiation set-up and lamps described in Section 2.2. Then, unirradiated (control) and irradiated-Tz were lysed in a 12.5% SDS-polyacrylamide gel electrophoresis (SDS-PAGE) sample buffer, electrophoresed and transferred on Polyvinylidene difluoride (PVDF) membrane (Thermo) activated previously with methanol. Non-specific binding sites were blocked with 5% non-fat-dried milk in TBS containing 0.05% Tween-20 (TBS-T). Membranes were incubated (1 h at room temperature) with different polyclonal primary antibodies, to analyze the damage on proteins localizated at tachyzoite's surface (mouse anti-SAG1, diluted at 1:500), micronemes (mouse anti-Mic1, a gift of Dubremetz, diluted at 1:500) and cytosol (rabbit anti-Hsp90 [20] and Hsp40 [21], diluted at 1:1000). Membranes were then washed with TBS-T prior to incubation with alkaline phosphatase-conjugated goat anti-rabbit or anti-mouse secondary antibodies (Sigma), diluted at 1:15,000. Immunoreactive protein bands were visualized by NBT-BCIP (Promega).

2.8. Intracellular ROS Analysis by H_2-DCF-DA Assay

Suspensions of 9×10^7 tachyzoites in 3 mL of PBS were first exposed to UVC, UVA or visible irradiation during different times. Aliquots of 1.8×10^6 unirradiated and irradiated-Tz were incubated with 2,7-dichlorodihydrofluoresceindiacetate 20 μM (H_2DCF-DA, Sigma) 30 min at 37 °C in a 5% CO_2 atmosphere and then put on ice in dark. Once inside the cells, this compound reacts with esterase-enzymes and ROS and becomes into DCF, a highly fluorescent molecule [22]. Samples were then examined using a BD FACSCalibur flow cytometer and data analysis was performed through FlowJo 7.6 software. 20,000 events were used for quantification of dichlorofluorescein (DCF) fluorescence. Cells were excited at 488 nm and DCF fluorescence was read on FL1 in linear scale. Samples were measured in triplicates, in three independent sets of experiments. Results are expressed as averaged smoothed (Savitzky-Golay) histograms and means of fluorescence intensities ± SEM *vs.* time of irradiation.

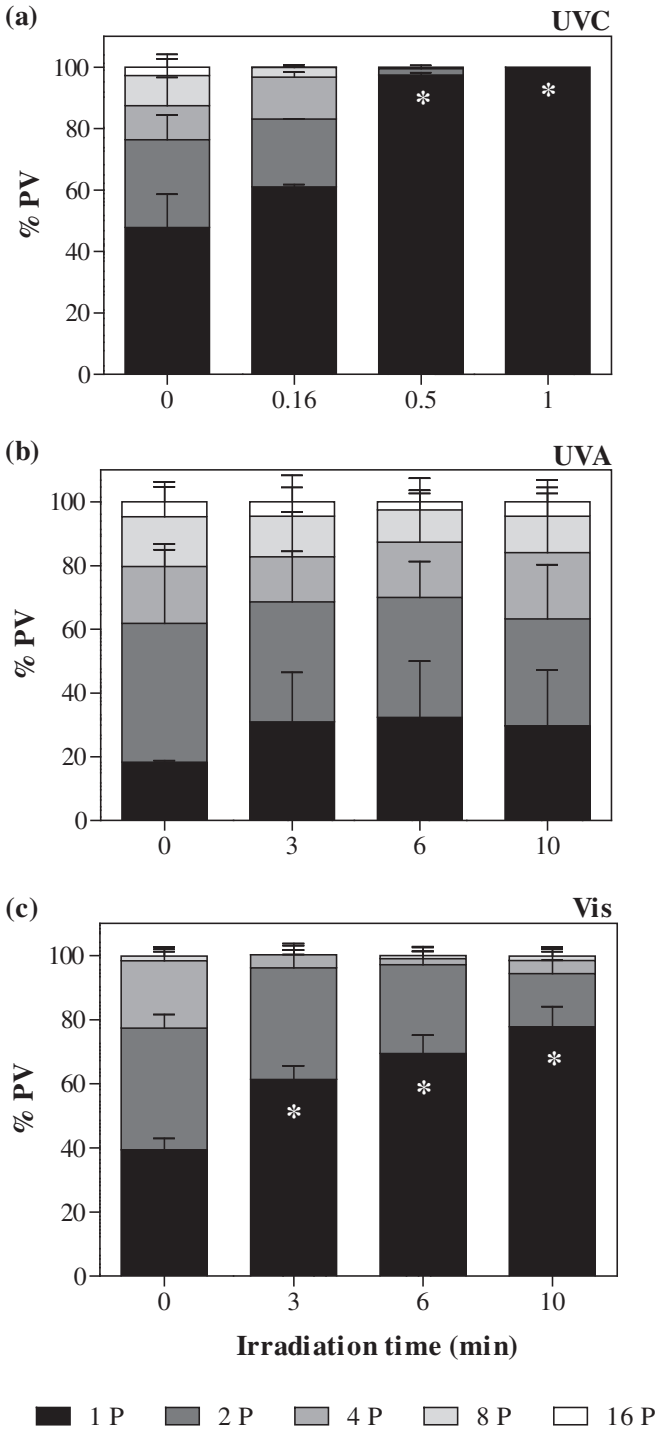

Fig. 2. Percentage of PV with 1, 2, 4, 8 or 16 tachyzoites (from black to white stacked bars, respectively) obtained after different times of (a) UVC, (b) UVA and (c) visible irradiation. Data correspond to 16 h post-infection. Results are expressed as means of % PV ± SEM from three independent experiments. (*) indicates significantly differences in % PV having one parasite between irradiated samples and control without irradiation ($p < 0.05$). ANOVA/Dunnett's tests were carried out as appropriate.

2.9. Growth Assay

To analyze the proliferation of treated parasites, 2.5×10^4 irradiated-Tz (420 nm), previously grown for two cycles in high PR DMEM were add to HFF monolayers grown in a 24 well plate. Because parasite growth is destructive to cell monolayers, infected cultures were followed daily by inverted microscope visualization until complete monolayer lysis along with the presence of extracellular tachyzoites or complete (host cell/tachyzoites) destruction as described [23].

2.10. DNA Relaxation Assay

An aqueous solution (pH 7.2, 3 mL) of supercoiled DNA (plasmid YFP28, 15.5 μg/mL) was irradiated (420 (± 20) nm, 1 cm of path length) in the presence of PR (50 μM). After exposure to radiation at variable time intervals, samples of 10 μL were analyzed by agarose-gel electrophoresis and data were treated following the procedure described elsewhere [24,25].

2.11. Statistical Analysis

All data were analyzed using GraphPad Prism 5.3 software. Means were compared using one-way ANOVA followed by Dunnett's post-test. When assumptions failed, Kruskal-Wallis one-way ANOVA on ranks followed by Dunn's method were performed. $p < 0.05$ was considered to be statistically significant when comparing the control and different irradiation times.

3. Results and Discussion

In order to analyze invasion ability in irradiated tachyzoites the number of PV per field was analyzed by IFA. Freshly lysed-out tachyzoites were irradiated with three different types of radiation (UVC, UVA and visible). Data depicted in Fig. 1a show that, in the whole irradiation time-scale tested, visible light had no effect, whereas UVC and UVA produced an inhibitory effect on parasite ability to infect host cells in a dose-dependent manner. Clearly, UVC induced the strongest effect: an almost full inhibition of invasion process was observed at 1 min of irradiation.

The decrease in the number of vacuoles per field induced by UVC and UVA might be a consequence of an inhibitory effect either on the attachment or on the invasion capability of the tachyzoites. Data obtained by red/green assay suggest that only invasion process was inhibited, since total amount of tachyzoites per field (internal plus attached) remained unaltered (see Fig. 1b, c and d), while internal tachyzoites per field decreased in a dose dependent manner.

On the other hand, in order to determine whether these types of radiation have any inhibitory effect on the parasite cycle processes, we measured the ability of intracellular-treated parasites to replicate. Since tachyzoites replicate only within the host cell by a process called endodiogeny, every round of replication results in a duplication of the parasite number *per* PV (*e.g.*, 2, 4, 8 and so on; Fig. SI.2) [26]. Every PV was generated from one parasite; therefore, the total number of tachyzoites inside the PV (2^n) indicates the number of replication events (n). Fig. 2 shows the percentage of PV that presented different numbers of tachyzoites. Note that an increase in % PV with only one parasite is the result of cell division inhibition.

UVC showed the strongest inhibitory effect: upon 0.5 min of irradiation 97.2% of the PV had just one parasite whereas upon 1 min of irradiation replication process was full inhibited (100% of PV contained one parasite, Fig. 2a). When parasites were exposed to UVA radiation, no significant effect on the parasite replication was observed, in the irradiation time-scale tested; *i.e.*, treated parasites showed the same replication trend as the untreated ones (Fig. 2b). On the other hand, visible light showed a slight inhibitory effect: the longer the irradiation time, the higher % PV with just one parasite (Fig. 2c). After 10 min irradiation under these conditions, 77.7% of PV contained just one parasite, which represents a 2-fold increase in cell division inhibition compared with control without irradiation (39.4% PV with one parasite).

The analysis of data presented in Fig. 2 in connection with results shown in Fig. 1 indicates that:

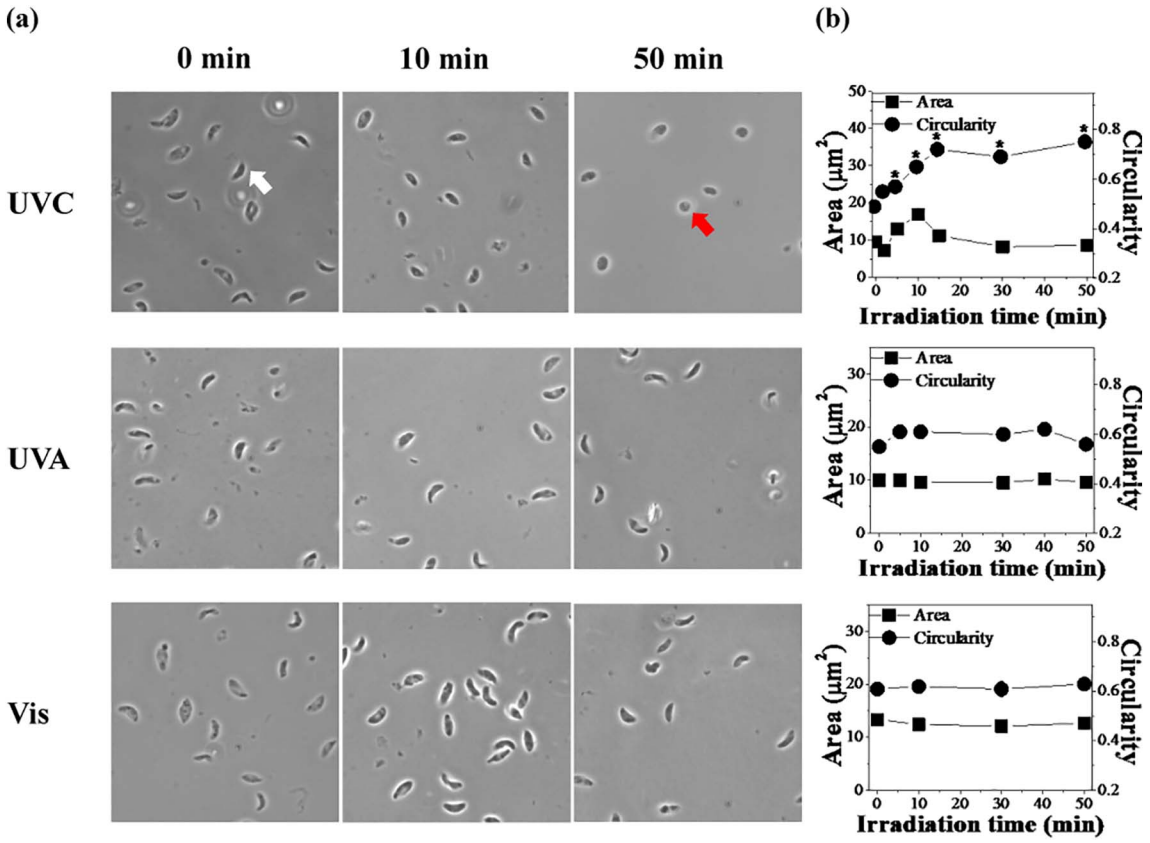

Fig. 3. (a) Phase-contrast images shown non-irradiated (*left column*) and irradiated samples (*middle* and *right columns*). (b) Circularity (right axis) and area (left axis) of parasites *vs.* irradiation time. Results are expressed as mean ± SEM from three independent experiments (*) indicates significantly statistical differences in circularity between irradiated samples and their respective controls without irradiation ($p < 0.05$, ANOVA/Dunnett's tests). (For interpretation of the references to colour in this figure, the reader is referred to the web version of this article.)

(i) At low doses (< 0.5 min) of irradiation, UVC induces a selective effect on parasite's replication. On the contrary, at high doses, UVC induces a full-non-selective damage affecting, in the same extent, both invasion and replication. This is quite logical since not only DNA but also proteins and other intracellular components are able to directly absorb the incident UVC radiation. Thus, selective parasite attenuation (*i.e.*, full inhibition of the replication without affecting the invasion capability) can only be achieved at very low doses of UVC.

These results are in agreement with those reported by Grimwood et al. [27] and Endo et al. [18] obtained > 30 years ago, using a quite different and not suitable methodology for parasites counting and also obtained under different experimental conditions (media or solvent). However, we do have substantial differences with the results very recently reported by with Kannan et al. [13], who achieved selective inhibition of replication process using relatively high doses of UVC (equivalent of > 21 min of irradiation under our experimental conditions). Although this, they only found humoral immune response in *in vivo* assays. In this case, authors adjudged the lack of cytokine production to the impaired invasion and/or replication of inactivated tachyzoites. We believe that under their experimental conditions, both invasion and replication are inhibited, leading to the lack of cellular immune response.

(ii) UVA exerts an inhibitory effect only on parasite invasion (statistically significant after 10 min of irradiation, $p < 0.05$), but not in replication process. All these facts rule out its potential use for an attenuation-based vaccine against *T. gondii*.

(iii) Visible light showed a significantly inhibitory effect only on the replication rate starting at 3 min ($p < 0.05$), resulting in a delay of one round of replication compared with the unirradiated-Tz. This fact suggests that visible radiation is selectively affecting or damaging those parasites organelles and/or functions related to the replication process (*vide infra*). The latter effect might be a consequence of photosensitized processes (see Discussion below).

Irradiated extracellular parasites were also analyzed by phase-contrast microscopy (Fig. 3). Qualitative and quantitative analyses of the images show that UVC induces serious changes in morphological aspects of the parasite (shape and size). Unirradiated-Tz show their normal crescent-shaped structure [28] (Fig. 3a, white arrow), whereas UVC irradiated-Tz show a quite high number of rounded parasites (Fig. 3a, red arrow). This is also evidenced by the rise in the calculated parameter circularity (Fig. 3b). In addition, average area of the parasites changes during the irradiation: at the beginning tachyzoites increase their sizes, may be due to an increase in the membrane permeability and at longer irradiation time parasites become smaller suggesting a loss of intracellular content. These results represent additional evidences of the full and non-selective damage induced by UVC. On the contrary, UVA and visible light showed no effect on both shape and size of tachyzoites.

It is well documented that UVC irradiation of proteins in both intracellular [29] and extracellular [30] conditions induces disruption of disulfide bonds. This photolysis may promote the formation of free thiols that can either be directly oxidized by UVC-induced ROS or create new disulfide cross-links (with possibly protein aggregation) [30]. Also, UV irradiation can induce photo-ionization and oxidation of aromatic amino acids [31]. Moreover, some results suggest that protein backbone is also damaged due to free radicals attack during UVC

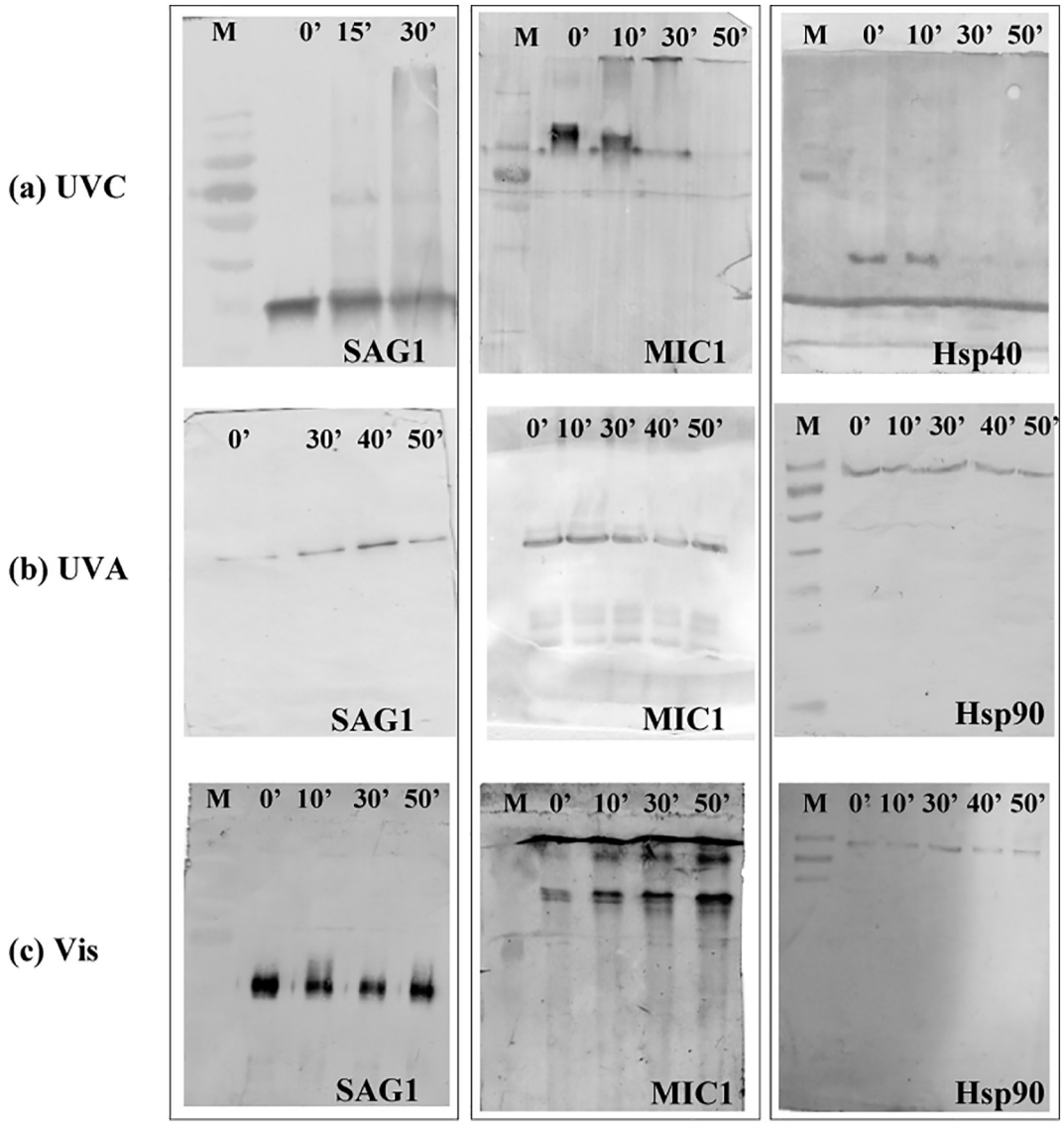

Fig. 4. Western-blots of representative membrane (SAG1), cytoplasmic (Hsp40 or Hsp90) and micronemal proteins (MIC1) irradiated during different irradiation times (0, 10, 30 and 50 min). (a), (b) and (c) correspond to UVC, UVA and visible treatments, respectively. Lane M represents the standard protein molecular-weight size marker.

exposure of cell cultures. However, UVA irradiation does not produce such protein modifications [29]. Additionally, irradiation of extracellular proteins with green and red visible lights make more packed ones [32].

Based on this background, the influence of the three irradiation sources used in the present work on electrophoretic behavior of certain proteins that can act as antigens was further investigated. Extracellular parasites were irradiated upon different intervals of time and were analyzed by Western-blot assay (Fig. 4). Three different types of proteins were monitored as representative examples of cytoplasmic (Hsp40 or Hsp90), membrane (SAG1) and microneme (Mic1, specialized secretory organelles highly relevant for gliding motility and host cell invasion) proteins.

Upon UVC treatment, all the tested proteins showed clear modifications. At high doses, some heavier bands appear (SAG1 and MIC1) and some others (Mic1 and Hsp40) are completely missed. This fact might be due to all radiation-induced processes described above. Moreover, it is worth mentioning that SAG1 [33] and MIC1 [34] have disulfide bonds. Therefore, photoinduced reactions initiated with S-S disruption might be observed. On the contrary, any evident effect on the investigated proteins was observed when UVA and visible light were used as excitation sources.

It is well known that UVC radiation can be directly absorbed by all the intracellular components of the parasites (*i.e.*, DNA, proteins, lipids, *etc.*). Therefore, this direct effect would certainly leads to irreversible modifications in those targets. Moreover, UV radiation stimulates ROS production inside different type of cells [29,35,36]. The generation of intracellular oxidative stress on irradiated-Tz was analyzed with H_2DCF-DA assay [22].

As is depicted in histograms of Fig. 5, measurable levels of intracellular ROS were not detected in samples exposed to UVA radiation. On the contrary, UVC radiation induced a marked generation of intracellular ROS in a dose-dependent manner. Such highly oxidant environment can, certainly, contribute to the overall damage on parasites morphology (proteins, membrane) and, consequently, on physiological processes such as invasion or replication. Additionally, a direct effect on superoxide dismutase and catalase enzymes, strongly related to the primary defense of the parasite against the harmful generation of ROS [37], could also contribute to the accumulation of these species.

On the other side, low but measurable levels of intracellular ROS were detected in samples exposed to visible light. This effect is further discussed below.

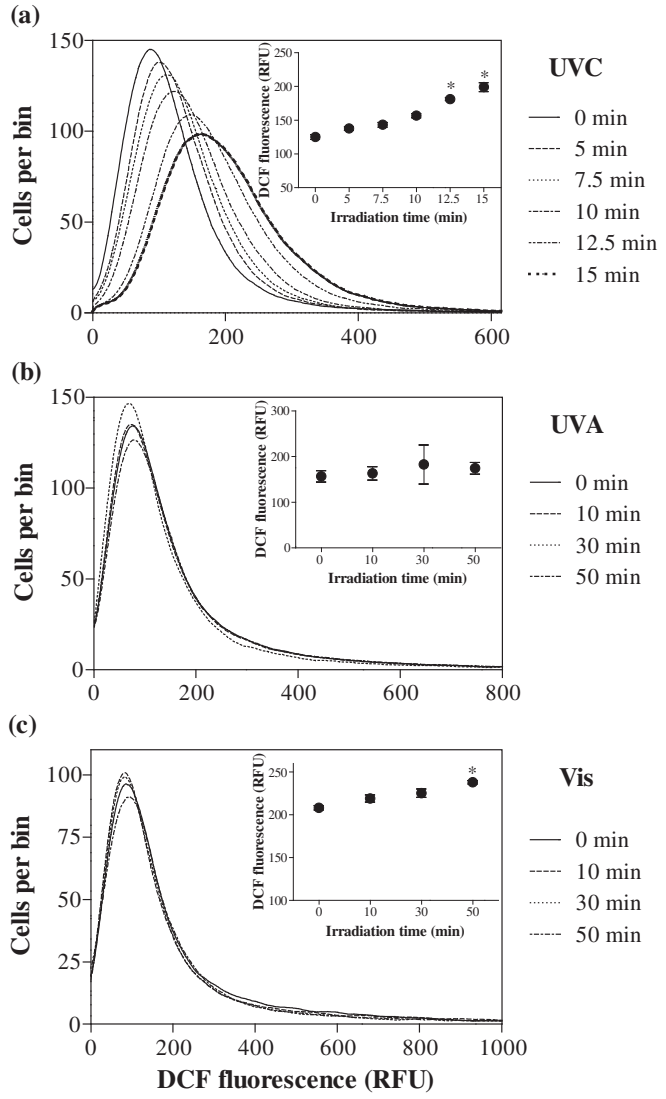

Fig. 5. Intracellular ROS production induced by (a) UVC, (b) UVA and (c) visible irradiation detected as DCF fluorescence by flow cytometry. Insets: Fluorescence mean (± SEM) for each radiation time. Results shown correspond to triplicates of one representative experiment. Data were analyzed by Kruskal-Wallis one-way ANOVA on ranks followed by Dunn's method (*indicates $p < 0.05$).

As it was described above, visible light induces a weak but selective effect on the parasite's replication (Figs. 1 and 2). Visible light is no longer absorbed by the main intracellular components such as DNA and proteins. Thus, the observed effects must be a consequence of photosensitized processes where endogenous and/or exogenous chromophores would act as photosensitizers when subject to visible light irradiation.

In all the described experiments parasites where irradiated in PBS solution, free of UVA and visible absorbing chromophores. However, tachyzoites were grown in DMEM containing PR as pH indicator. Therefore, PR could certainly be accumulated into the host cell and, consequently, into the parasites. PR shows a quite high relative absorption coefficient in the visible region of the electromagnetic spectra. Moreover, under physiological pH, the acidic species of PR shows its maxima of absorption centered at ~420 nm (Fig. SI.3). Although quite inefficient, PR is a photoactive compound. E. g., under photoexcitation with a sunlight simulator, in aqueous solution, PR follows a hydroxyl radical-mediated photochemical degradation [38]. Also, it was found to be phototoxic for human keratinocyte cell lines when subject to solar-simulated radiation [39]. Moreover, we proved the capability of PR to photoinduce damage on DNA under our irradiation conditions (Fig. SI.4).

In this context, the photosensitized effect of PR on the parasite's invasion and replication rates, upon visible irradiation, was additionally evaluated. For this purpose, three independent sets of parasites were grown in DMEM media containing three different PR concentrations (0, 0.04 and 0.40 mM, respectively) (see Experimental Section 2.2.2).

Results depicted in Fig. 6 show that, although invasion rates were not affected (see Fig. 6a), PR clearly exert an effect on the replication rate of irradiated-Tz in a dose-dependent manner. Briefly, upon irradiation, tachyzoites grown in the absence of PR did not show any decrease in replication process with respect to the unirradiated-Tz (Fig. 6b). However, in presence of PR a significant delay in replication rates was observed after 30 min of irradiation (Fig. 6c and d). This is particularly evident when comparing data obtained upon 50 min of irradiation, where the relative percent of PV with one parasite observed were 4.2, 41.1 and 73.9% for PR concentrations of 0, 0.04 and 0.4 mM, respectively (Fig. 6). In consequence, one can conclude that PR is the photosensitizer playing a key role in the selective attenuation observed on tachyzoites when subject to visible irradiation.

In this point, it is relevant to recall the distinctive effect induced by PR on parasites when subject to UVA with respect to visible irradiation (Figs. 1 and 2). Briefly, even in the presence of PR, UVA exerts an inhibitory effect only on parasite's invasion capability. Taking into account the quite low relative absorption coefficient of PR at 365 nm, in aqueous solution at physiological pH (Fig. SI.3), one can conclude that results obtained under UVA irradiation would be due to other endogenous photosensitizers rather than PR.

Growth assay was also performed to further evaluate the photosensitized effect of PR on tachyzoites. Specifically, we used both tachyzoites grown in commercial DMEM (0.04 mM of PR) as control populations (ctrl-Tz), as well as unirradiated and irradiated PR-loaded-Tz (*i.e.*, tachyzoites previously grown in high PR DMEM, 0.40 mM). Treated-Tz was then added to HFF monolayers (Section 2.9).

Ctrl-Tz and unirradiated-PR-loaded-Tz (0 min) showed that HFF monolayers were completely destroyed in 6 and 7 days, respectively (see discussion below). However, irradiated-PR-loaded-Tz clearly showed a delay in the lysis of host cells in a dose-dependent manner (Fig. 7 and Table SI.1). Note that total monolayer destruction was not observed, along the time period of the experiments (20 days), when the highest dose of visible light was applied (50 min).

It is also important to note that PR exerts an effect in culture cells. Because of its estrogen receptor stimulator property [40] it promotes cell proliferation in different cell lines [41–44] and the differentiation of bone marrow stromal cells [45]. Additionally, abnormal epileptiform-like bursting activities are observed in neurons in hippocampal cultures when PR is absent [46]. It has also been reported that phenol red is toxic for HeLa cells after being adsorbed and delivered into cells by carbon nanoparticles (CNPs) in a serum-free cell culture medium [47].

Under our experimental conditions, a delay in the lysis of infected Vero cell monolayers (induced by *T. gondii*) was observed when tachyzoites and cells were grown in DMEM media with the highest PR concentration (0.40 mM), with respect to PR-free and commercial DMEM media. Such a delay could certainly be a consequence of: (i) a direct effect of PR on parasites metabolism or (ii) a potential increase in the number of host cells that might be stimulated by PR.

To further investigate the above hypotheses, 3×10^4 Vero cells were grown during six days in normal and high PR DMEM (0.04 and 0.4 mM, respectively), both supplemented with 10% of FBS. Then, cells were harvested and counted by Neubauer chamber. Data obtained herein showed no distinctive effect on the proliferation of host cells between the two set of experiments (see Fig. SI. 5). These results are in good agreement with those obtained with other culture cells [42].

The above described data reveal that, in the absence of light, PR also

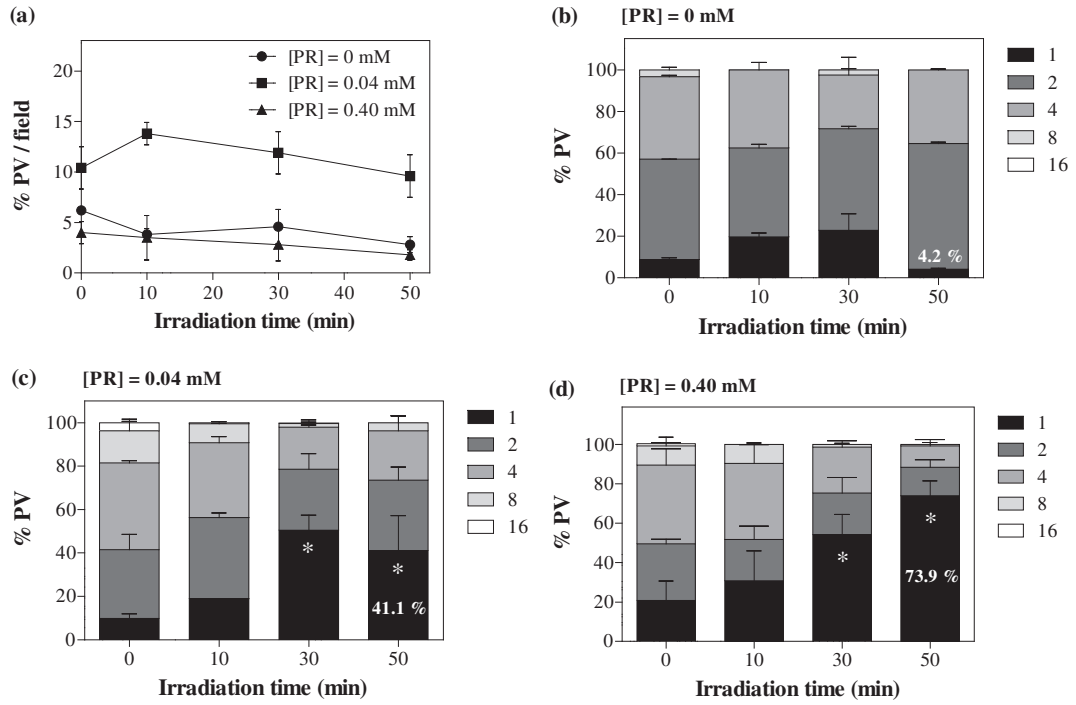

Fig. 6. Irradiation (420 nm) of tachyzoites grown in DMEM media containing 0,0.04 and 0.4 mM of PR: Effects on (a) invasion rate. Non-significant statistical differences were found (ANOVA/Dunnett's tests, $p < 0.05$). (b), (c) and (d) replication rate (24 h post-infection). (b), (c) and (d) correspond to 0, 0.04 and 0.40 mM of PR respectively. Results are expressed as mean ± SEM from three independent experiments (*) indicates significantly differences between irradiated samples and control without irradiation ($p < 0.05$, ANOVA/Dunnett's tests).

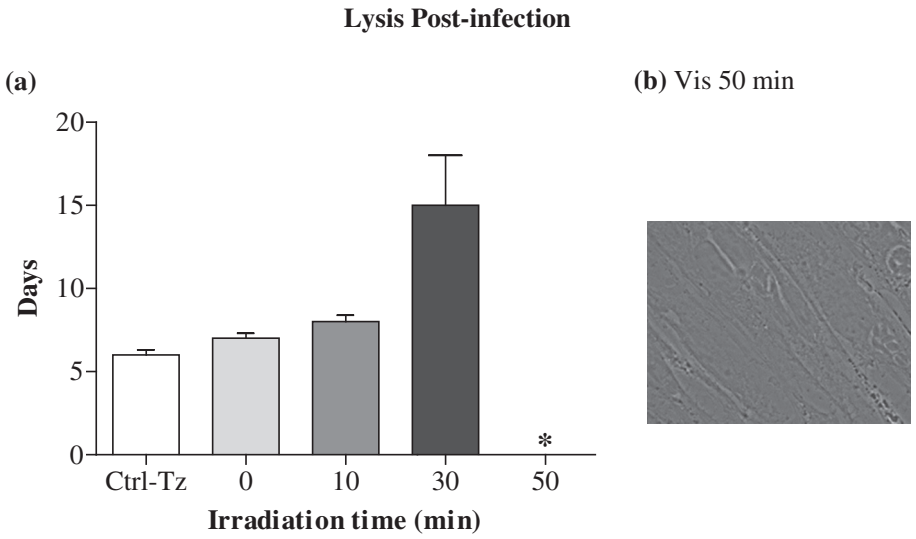

Fig. 7. Growth assay of irradiated-PR-loaded-Tz (λ_{exc} = 420 nm) during different times. *Total monolayer lysis was not observed 20 days post-infection. Data obtained from three independent experiments (± SD). (b) Phase-contrast image of HFF cells observed 20 days after infection with irradiated-PR-loaded-Tz (time of irradiation = 50 min).

induces a direct effect on *T. gondii* yielding a delay in the monolayer lysis, most probably, due to an effect on parasite replication mechanisms. The same trend was observed in growth assay when comparing results obtained from Ctrl-Tz and unirradiated-PR-loaded-Tz (Fig. 7 and Table SI.1).

4. Conclusions

When considering all the material provided herein, four key points may be highlighted:

(i) UVC is clearly a quite invasive and destructive excitation source, affecting both the invasion and the replication capability of the parasite. Antigens presented by UVC-attenuated parasites would be seriously modified both from structural and chemical point of view. In view of live-attenuated vaccines production, UVC would not be a suitable irradiation source. However, when comparing with γ-radiation, UVC is a cheap and safe sterilizing method.

(ii) UVA radiation affects only invasion process due to the effect of endogenous photosensitizers.

(iii) Visible light showed the desired selective effect, *i.e.*, inhibition of the replication capability of the parasite without affecting the invasion. The latter effect might only take place through photosensitized processes, where phenol red (PR) seems to play a key role. In this context it is worth mentioning that, although PR is not an efficient photosensitizer, it might serve as a proof of concept and a stepping stone in the search for selective attenuation methods.

Since attenuated parasites conserve their infectiveness, the methodology presented herein might be potentially implemented to

study the role of immune activation following *T. gondii* infections. Furthermore, the photosensitized attenuation method might be applicable to any *T. gondii* strain and/or other types of obligate intracellular parasites. Thus, differences in parasite-strain immune activation can be studied. In addition, in the search of novel strategies for the development of live-attenuated vaccines against intracellular parasites, photosensitizing processes, triggered by visible light, seems to be a quite promising alternative.

(iv) In the absence of light, PR also induces a mild and reversible effect on *T. gondii* replication capability. Taking into account that PR is widely used in cell culture applications; its potential influence and/or interference on biological experiments has to be considered.

Acknowledgements

The present work was partially supported by CONICET (PIP 00400), ANPCyT (PICT 2012-0423, 2014-2856 and 2015-0374) and UNSAM (28/E122 and PUE 16/14). F.M.C (Researcher), S.O.A. (Researcher), M.M.C. (Researcher), V.M.C (Researcher), J.G.Y. (Fellow), M.L.A (Fellow) and A.M.A. (Fellow) are members of National Research Council of Argentina (CONICET). Authors deeply thank C. G. Alberici (CONICET) and A. Ganuza (CIC) for their technical support.

Appendix A. Supplementary Data

Supplementary data to this article can be found online at https://doi.org/10.1016/j.jphotobiol.2017.10.008.

References

[1] J. Remington, Toxoplasmic encephalitis in AIDS, Clin. Infect. Dis. 15 (1992) 211–222.
[2] J.G. Montoya, O. Liesenfeld, Toxoplasmosis, Lancet 363 (2004) 1965–1976.
[3] J.L. Jones, J.P. Dubey, Foodborne toxoplasmosis, Clin. Infect. Dis. 55 (2012) 845–851.
[4] C.A. Hunter, L.D. Sibley, Modulation of innate immunity by *Toxoplasma gondii* virulence effectors, Nat. Rev. Microbiol. 10 (2012) 766–778.
[5] M. Montazeri, M. Sharif, S. Sarvi, S. Mehrzadi, E. Ahmadpour, A. Daryani, A systematic review of in vitro and in vivo activities of anti-toxoplasma drugs and compounds (2006–2016), Front. Microbiol. 8 (2017) 25.
[6] D. Buxton, E.A. Innes, A commercial vaccine for ovine toxoplasmosis, Parasitology 110 (1995) S11–S16.
[7] J. Kur, L. Holec-Gąsior, E. Hiszczyńska-Sawicka, Current status of toxoplasmosis vaccine development, Expert Rev. Vaccines 8 (2009) 791–808.
[8] R.A. Seder, L.-J. Chang, M.E. Enama, K.L. Zephir, U.N. Sarwar, I.J. Gordon, L.A. Holman, E.R. James, P.F. Billingsley, A. Gunasekera, A. Richman, S. Chakravarty, A. Manoj, S. Velmurugan, M. Li, A.J. Ruben, T. Li, A.G. Eappen, R.E. Stafford, S.H. Plummer, C.S. Hendel, L. Novik, P.J.M. Costner, F.H. Mendoza, J.G. Saunders, M.C. Nason, J.H. Richardson, J. Murphy, S.A. Davidson, T.L. Richie, M. Sedegah, A. Sutamihardja, G.A. Fahle, K.E. Lyke, M.B. Laurens, M. Roederer, K. Tewari, J.E. Epstein, B.K.L. Sim, J.E. Ledgerwood, B.S. Graham, S.L. Hoffman, V.R.C.S.T., the, Protection against malaria by intravenous immunization with a nonreplicating sporozoite vaccine, Science 341 (2013) 1359–1365.
[9] D. Rivier, R. Shah, P. Bovay, J. Mauel, Vaccine development against cutaneous leishmaniasis. Subcutaneous administration of radioattenuated parasites protects CBA mice against virulent *Leishmania* major challenge, Parasite Immunol. 15 (1993) 75–84.
[10] S. Datta, M. Manna, S. Khanra, M. Ghosh, R. Bhar, A. Chakraborty, S. Roy, Therapeutic immunization with radio-attenuated Leishmania parasites through i.m. route revealed protection against the experimental murine visceral leishmaniasis, Parasitol. Res. 111 (2012) 361–369.
[11] G.J. Vos, P.R. Gardiner, Parasite-specific antibody responses of responses of ruminants infected with *Trypanosoma vivax*, Parasitology 100 (1990) 93–100.
[12] M. Assmar, M. Hajizadeh Manjili, A.R. Esmaeili-Rastaghi, M. Farahmand, N. Piazak, S. Rafati, S.R. Naddaf Dezfooli, Immunogenicity of gamma-irradiated *Toxoplasma gondii* tachyzoites in mice, Iran. Biomed. J. 3 (1999) 93–97.
[13] G. Kannan, E. Prandovszky, C.B. Steinfeldt, K.L. Gressitt, C. Yang, R.H. Yolken, E.G. Severance, L. Jones-Brando, M.V. Pletnikov, One minute ultraviolet exposure inhibits *Toxoplasma gondii* tachyzoite replication and cyst conversion without diminishing host humoral-mediated immune response, Exp. Parasitol. 145 (2014) 110–117.
[14] A. Dumètre, C. Le Bras, M. Baffet, P. Meneceur, J.P. Dubey, F. Derouin, J.-P. Duguet, M. Joyeux, L. Moulin, Effects of ozone and ultraviolet radiation treatments on the infectivity of *Toxoplasma gondii* oocysts, Vet. Parasitol. 153 (2008) 209–213.
[15] B.A. Fox, D.J. Bzik, Nonreplicating, cyst-defective type II *Toxoplasma gondii* vaccine strains stimulate protective immunity against acute and chronic infection, Infect. Immun. 83 (2015) 2148–2155.
[16] S. Ramamoorthy, D.S. Lindsay, G.G. Schurig, S.M. Boyle, R.B. Duncan, R. Vemulapalli, N. Sriranganathan, Vaccination with γ-irradiated *Neospora caninum* tachyzoites protects mice against acute challenge with *N. caninum*, J. Eukaryot. Microbiol. 53 (2006) 151–156.
[17] A. Wales, J.R. Kusel, Biochemistry of irradiated parasite vaccines: suggested models for their mode of action, Parasitol. Today 8 (1992) 358–363.
[18] T. Endo, B. Pelster, G. Piekarski, Infection of murine peritoneal macrophages with *Toxoplasma gondii* exposed to ultraviolet light, Z. Parasitenkd. 65 (1981) 121–129.
[19] K.W. Straub, E.D. Peng, B.E. Hajagos, J.S. Tyler, P.J. Bradley, The moving junction protein RON8 facilitates firm attachment and host cell invasion in *Toxoplasma gondii*, PLoS Pathog. 7 (2011) e1002007.
[20] P.C. Echeverria, M. Matrajt, O.S. Harb, M.P. Zappia, M.A. Costas, D.S. Roos, J.F. Dubremetz, S.O. Angel, *Toxoplasma gondii* Hsp90 is a potential drug target whose expression and subcellular localization are developmentally regulated, J. Mol. Biol. 350 (2005) 723–734.
[21] M.J. Figueras, O.A. Martin, P.C. Echeverria, N. de Miguel, A. Naguleswaran, W.J. Sullivan Jr., M.M. Corvi, S.O. Angel, *Toxoplasma gondii* Sis1-like J-domain protein is a cytosolic chaperone associated to HSP90/HSP70 complex, Int. J. Biol. Macromol. 50 (2012) 725–733.
[22] A. Gomes, E. Fernandes, J.L. Lima, Fluorescence probes used for detection of reactive oxygen species, J. Biochem. Biophys. Methods 65 (2005) 45–80.
[23] M.L. Alomar, F.A. Rasse-Suriani, A. Ganuza, V.M. Cóceres, F.M. Cabrerizo, S.O. Angel, In vitro evaluation of β-carboline alkaloids as potential anti-toxoplasma agents, BMC. Res. Notes 6 (2013) 193.
[24] M.M. Gonzalez, M. Vignoni, M. Pellon-Maison, M.A. Ales-Gandolfo, M.R. Gonzalez-Baro, R. Erra-Balsells, B. Epe, F.M. Cabrerizo, Photosensitization of DNA by beta-carbolines: kinetic analysis and photoproduct characterization, Org. Biomol. Chem. 10 (2012) 1807–1819.
[25] M.M. Gonzalez, M. Pellon-Maison, M.A. Ales-Gandolfo, M.R. Gonzalez-Baro, R. Erra-Balsells, F.M. Cabrerizo, Photosensitized cleavage of plasmidic DNA by norharmane, a naturally occurring beta-carboline, Org. Biomol. Chem. 8 (2010) 2543–2552.
[26] B. Striepen, C.N. Jordan, S. Reiff, G.G. van Dooren, Building the perfect parasite: cell division in *Apicomplexa*, PLoS Pathog. 3 (2007) e78.
[27] B.G. Grimwood, Infective *Toxoplasma gondii* trophozoites attenuated by ultraviolet irradiation, Infect. Immun. 28 (1980) 532–535.
[28] J.P. Dubey, D.S. Lindsay, C.A. Speer, Structures of *Toxoplasma gondii* tachyzoites, bradyzoites, and sporozoites and biology and development of tissue cysts, Clin. Microbiol. Rev. 11 (1998) 267–299.
[29] S.R. Panikkanvalappil, S.M. Hira, M.A. El-Sayed, Elucidation of ultraviolet radiation-induced cell responses and intracellular biomolecular dynamics in mammalian cells using surface-enhanced Raman spectroscopy, Chem. Sci. 7 (2016) 1133–1141.
[30] H.L. Chan, P.R. Gaffney, M.D. Waterfield, H. Anderle, H. Peter Matthiessen, H.P. Schwarz, P.L. Turecek, J.F. Timms, Proteomic analysis of UVC irradiation-induced damage of plasma proteins: serum amyloid P component as a major target of photolysis, FEBS Lett. 580 (2006) 3229–3236.
[31] D.I. Pattison, A.S. Rahmanto, M.J. Davies, Photo-oxidation of proteins, Photochem. Photobiol. Sci. 11 (2012) 38–53.
[32] J.H. Espinoza, E. Reynaga-Hernandez, J. Ruiz-Garcia, G. Montero-Moran, M. Sanchez-Dominguez, H. Mercado-Uribe, Effects of green and red light in betaL-crystallin and ovalbumin, Sci Rep 5 (2015) 18120.
[33] F. Velge-Roussel, T. Chardès, P. Mévélec, M. Brillard, J. Hoebeke, D. Bout, Epitopic analysis of the *Toxoplasma gondii* major surface antigen SAG1, Mol. Biochem. Parasitol. 66 (1994) 31–38.
[34] M.N. Fourmaux, A. Achbarou, O. Mercereau-Puijalon, C. Biderre, I. Briche, A. Loyens, C. Odberg-Ferragut, D. Camus, J.F. Dubremetz, The MIC1 microneme protein of *Toxoplasma gondii* contains a duplicated receptor-like domain and binds to host cell surface, Mol. Biochem. Parasitol. 83 (1996) 201–210.
[35] M. Widel, A. Krzywon, K. Gajda, M. Skonieczna, J. Rzeszowska-Wolny, Induction of bystander effects by UVA, UVB, and UVC radiation in human fibroblasts and the implication of reactive oxygen species, Free Radic. Biol. Med. 68 (2014) 278–287.
[36] D.E. Heck, A.M. Vetrano, T.M. Mariano, J.D. Laskin, UVB light stimulates production of reactive oxygen species: unexpected role for catalase, J. Biol. Chem. 278 (2003) 22432–22436.
[37] L. David Sibley, R. Lawson, E. Weidner, Superoxide dismutase and catalase in *Toxoplasma gondii*, Mol. Biochem. Parasitol. 19 (1986) 83–87.
[38] J. Hay, W. Khan, J.K. Sugden, Photochemical decomposition of phenol red (phenolsulphonphthalein), Dyes Pigments 24 (1994) 305–312.
[39] A. Maguire, B. Morrissey, J.E. Walsh, F.M. Lyng, Medium-mediated effects increase cell killing in a human keratinocyte cell line exposed to solar-simulated radiation, Int. J. Radiat. Biol. 87 (2011) 98–111.
[40] V.C. Jordan, A.C. Tate, S.D. Lyman, B. Gosden, M.F. Wolf, R.R. Bain, W.V. Welshons, Rat uterine growth and induction of progesterone receptor without estrogen receptor translocation, Endocrinology 116 (1985) 1845–1857.
[41] M. Ernst, C. Schmid, E.R. Froesch, Phenol red mimics biological actions of estradiol: enhancement of osteoblast proliferation in vitro and of type I collagen gene expression in bone and uterus of rats in vivo, J. Steroid Biochem. 33 (1989) 907–914.
[42] Y. Berthois, J.A. Katzenellenbogen, B.S. Katzenellenbogen, Phenol red in tissue culture media is a weak estrogen: implications concerning the study of estrogen-responsive cells in culture, Proc. Natl. Acad. Sci. 83 (1986) 2496–2500.
[43] J. Węsierska-Gądek, T. Schreiner, M. Maurer, A. Waringer, C. Ranftler, Phenol red in the culture medium strongly affects the susceptibility of human MCF-7 cells to roscovitine, Cell. Mol. Biol. Lett. 12 (2007) 280–293.
[44] J. Węsierska-Gądek, T. Schreiner, M. Gueorguieva, C. Ranftler, Phenol red reduces

ROSC mediated cell cycle arrest and apoptosis in human MCF-7 cells, J. Cell. Biochem. 98 (2006) 1367–1379.
[45] K. Still, L. Reading, A. Scutt, Effects of phenol red on CFU-f differentiation and formation, Calcif. Tissue Int. 73 (2003) 173–179.
[46] X. Liu, B. Chen, L. Chen, W.T. Ren, J. Liu, G. Wang, W. Fan, X. Wang, Y. Wang, U-shape suppressive effect of phenol red on the epileptiform burst activity via activation of estrogen receptors in primary hippocampal culture, PLoS One 8 (2013) e60189.
[47] Y. Zhu, X. Zhang, J. Zhu, Q. Zhao, Y. Li, W. Li, C. Fan, Q. Huang, Cytotoxicity of phenol red in toxicity assays for carbon nanoparticles, Int. J. Mol. Sci. 13 (2012) 12336–12348.